Modelling of the Bolted Joint in Relation to the Working Load of the Bolt

RAFAŁ GRZEJDA
Faculty of Mechanical Engineering and Mechatronics,
West Pomeranian University of Technology in Szczecin,
19 Piastow Ave., 70-310 Szczecin,
POLAND

Abstract: - The paper presents a piece of research carried out on the development of modelling and calculation methods for multi-bolted connections. The influence of the modelling of the separated bolted joint on the value of the working load in the bolt was considered. A stiffness analysis of the bolted joint for selected linear and non-linear models was carried out. Guidelines for the selection of the modelling method for the analysis of working loads occurring in a bolted joint are discussed.

Key-Words: - bolted joint, working load, bolt load, bolt model, stiffness analysis, FE analysis.

Received: April 25, 2024. Revised: November 5, 2024. Accepted: December 12, 2024. Published: January 28, 2025.

1 Introduction

A fundamental task to be solved at the beginning of the design process of mechanical structures is to find a compromise between the level of assumptions of the adopted solid and computational models and the required accuracy of the computational results to be produced, [1], [2], [3]. This is particularly the case for systems composed of multiple contacting components, of which multi-bolted connections are an example, [4], [5]. At the same time, some difficulties arise when modelling multi-bolted connections with any geometry of the elements being joined and loaded in any way, [6]. Therefore, this paper undertakes to investigate the issue of modelling a single-bolted joint, separated from a multi-bolted connection, as less complex in its design.

The most important simplifications regarding the modelling of bolted joints are related to the way the fasteners are represented in the joint. Restricting considerations to modelling by the finite element method (FEM), fasteners can be modelled as:

- preload, without the contribution of the fastener model, [7], [8],
- full restraint of nodes, without the contribution of the fastener model, [9],
- two-nodes connector with kinematic couplings, [10],
- rigid shank with coupling constraints, [11],
- spring elements, [12], [13],
- rod elements, [14],
- bolt head, with no involvement of the other parts of the fastener, [15],
- beam elements, [16], [17],
- rigid bolt head and a rigid nut connected by a deformable beam, [18], [19], [20],
- substitute hybrid models, [21], [22],
- solid model with non-deformable bolt head, [23],
- solid model built from a substitute material model, [24],
- solid model without mapping of the thread outline, [25], [26], [27],
- solid model with mapping of the thread outline, [28], [29], [30].

There are also publications that analyse structural models without taking into account the occurrence of bolted joints that are present in the mapped real object, [31], [32].

With the above list in mind, different fastener models are allowed depending on the modelling and calculation objective of the bolted joint model. In this paper, the main objective is to determine the stiffness of the connected elements in a bolted joint, so the fastener is modelled using the first of the above-mentioned methods, i.e. as a preload (force load applied to the fastened components, [33]).

The second group of simplifications regarding the modelling of bolted joints is related to the way in which the elements to be connected and their contact are represented in the joint. In some works, the connected elements have been modelled as rigid elements, [34], [35]. However, limiting the consideration to modelling by means of FEM, the connected elements are mostly treated as deformable. However, the contact joint between them can be modelled as:

- rigid joint, [18], [36],
- deformable linear joint, [6],
- deformable non-linear joint, [19].

Of the aforementioned ways of modelling the contact layer between the elements connected in a bolted joint, for the purpose of the comparative analyses in this paper, the modelling of the contact as a rigid joint and as a deformable non-linear joint was chosen.

In the last five years, the literature on the modelling of multi-bolted connections and bolted joints has been expanded by many new publications. The results of numerical study of angle members connected by one leg with one row of bolts were presented in [37]. The effect of thermal expansion on the residual bolt preload force at the flange connection in the body of a high-pressure turbine was examined in [38]. Tests on bolted composite-metal connections to predict the bearing load and to simulate the failure behaviour were conducted in [39]. The static strength of friction-type high-strength bolted T-stub connections in shear and compression was investigated in [40]. The results of evaluating the reliability of connections with slip-critical bolts and fillet welds in combination were showed in [41]. Predicting the service life of a gasket operating in a bolted flange connection subjected to cyclic bending was the subject of [42]. The load and stress distribution of a bolted composite connection loaded with shear forces was analysed in [43]. Bolted foundation flange connections at different configurations were studied in [44]. The steel flush and extended end-plate connections in a column loss scenario were parametrically investigated in [45]. A thermal analysis of an example bolted joint was performed in [46]. The results of a test of a stiffened angle connection in the auxiliary axis were described in [47]. The seismic behaviour of concentrically braced steel frames with extended bolted end plate connections was studied in [48].

The exemplary publications cited above relate to simple joint strength analyses aimed at demonstrating either some behaviour or the compatibility of the models with the objects they represent. In contrast, this paper proposes a systematic approach to the modelling of multi-bolted connections. The essence of the proposed modelling approach is to treat the multi-bolted connection as a system composed of three sub-systems: a set of bolts, a body component and a non-linear contact layer between the body component and the non-deformable support. Thanks to the systematic approach, it is possible to continuously develop the method by generalising the models of the individual sub-systems that form the connection.

To summarise the introduction, considerations are limited in this paper to the study of the effect of the modelling and simplification of a single bolted joint on the value of the working load in the bolt.

2 Fundamentals of Analysis

In the literature on the fundamentals of machine design, [49], [50] the generally known Rötscher model (Figure 1) is proposed for the calculation of the elasticity of the individual elements of a bolted joint, in which:

- linear elasticity of the bolt, [51], and the joined components is assumed,
- presence of a contact layer between the components to be joined is omitted,
- elasticity of the bolt is determined directly from the Hooke's formula for uniaxial compression, [52],
- elasticity of the joined components is also calculated from Hooke's formula for an equivalent sleeve replacing the load-bearing zone (approximately equal to the volume of a pair of hollow truncated cones joined by their bases, [53], Figure 1(a)).

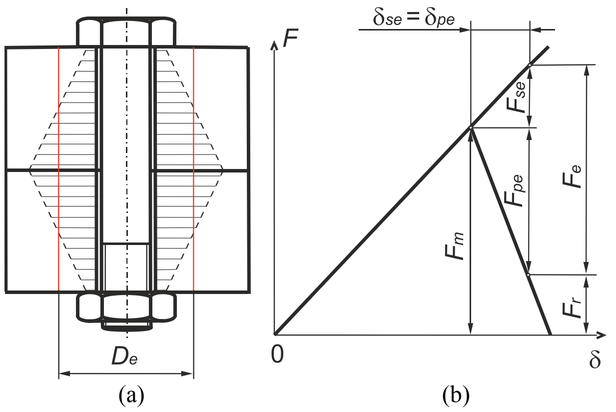

Fig. 1: Model of the bolted joint: a) influence cones and equivalent sleeve with diameter D_e, b) elasticity diagram of the joint (F_m – preload, F_e – service load, F_r – residual clamp, F_{se} – increase in the bolt force due to service load, F_{pe} – increase in the force in joined components due to service load, δ_{se} – deformation of the bolt under service load, δ_{pe} – deformation of joined components under service load)

Using the relationships derived from the elasticity diagram (Figure 1(b)), the value of the working load in the bolt, F_s, can be determined as:

$$F_s = F_m + F_{se} \quad (1)$$

The value of the force F_{se} can be calculated from the formula:

$$F_{se} = \alpha \cdot F_m \cdot \frac{c_s}{c_p + c_s} \quad (2)$$

where: α – percentage increase in the service load in relation to the preload, c_s – stiffness of the bolt, c_p – stiffness of the joined components.

Further modifications of the model presented above have been extensively discussed in [54], [55], and mainly concern the way in which the shape and volume of the load influence area in the joined components, exerted by the bolt head and nut, or the way in which the service force is applied, is determined. Based on a comparison of these models, it can be concluded that:

- using the formulas derived, the correct results of the bolt elasticity calculations are obtained,
- existing methods for calculating the elasticity of joined components have been aimed at specific areas of application and therefore do not have the characteristics of universality, so that calculations using them often lead to different results and differ from experimental findings.

With the latter conclusion in mind, it should be noted that a better way to determine the elasticity of the bolted joint components is to use FEM. Work on this issue has usually neglected the flexibility of the contact layer between the components to be joined, [54], [56].

In order to analyse the aforementioned methods of determining the elasticity of the connected components of a bolted joint, calculations were carried out for three types of models:

- VDI – established according to the assumptions of the VDI 2230 standard, [55],
- FEM-L – FEM-based model without contact layer between joined components (linear model),
- FEM-NL – FEM-based model with a contact layer between joined components (non-linear model).

3 Computational Models

The subject of the study is a bolted joint, separated from a larger multi-bolted connection. The system under consideration is assumed to be a component with the dimensions shown in Figure 2, resting on a non-deformable support.

The calculations were made for the flange thickness $h \in \{20\ \text{mm}, 40\ \text{mm}, 80\ \text{mm}\}$. The fastener in the joint is an M10 bolt made to mechanical property class 8.8. The preload value F_m = 20 kN was selected on the basis of PN-EN 1591-1, [57]. Meanwhile, the surface area A_m = 80π mm^2, on which the preload value F_m was applied, was determined on the basis of PN-EN ISO 7091, [58].

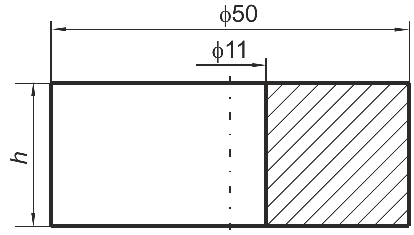

Fig. 2: Flange geometry

The contact zone between the flange and the non-deformable support (in the case of the FEM-NL model) was replaced by a conventional Winkler-type elastic layer, described by a set of one-sided springs, [59]. The following relation, determined experimentally, was adopted as the non-linear characteristics of these springs:

$$p = 3.428 \cdot \delta^{1.657} \quad (3)$$

where: p – normal surface pressure, δ – normal contact deformation.

The means of restraint and loading for the finite element models (FEM L and FEM N) are shown in Figure 3(a) and Figure 3(b) respectively. In the flange model without a contact layer, all degrees of freedom at the interface between the flange and the non-deformable support were taken away. In the model of the flange resting on a non-linear foundation, the flange was restrained by taking away degrees of freedom in directions perpendicular to the axis of symmetry of the flange, at the nodes lying on the side of the flange cylinder, while the non-linear springs were taken away degrees of freedom in the Z-axis direction (parallel to the axis of symmetry of the flange), at the nodes lying at the contact of the springs with the non-deformable support.

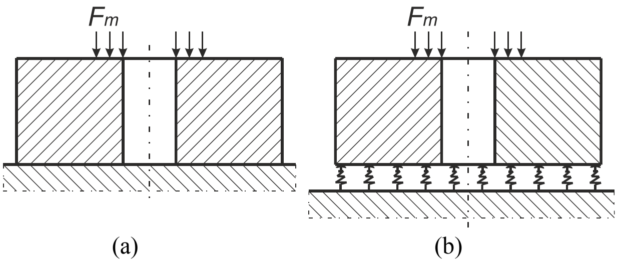

Fig. 3: Boundary conditions for models: a) FEM-L, b) FEM-NL

The calculation of the flange models in FEM convention was carried out using ANSYS, [60]. For the construction of the flange models, the following were used:

- 8-node 3D elements - Solid 45 (FEM-L model and FEM-NL model),
- non-linear springs - Combin 39 (FEM-NL model).

An example of an FEM L-type flange model (for $h = 20$ mm) is shown in Figure 4.

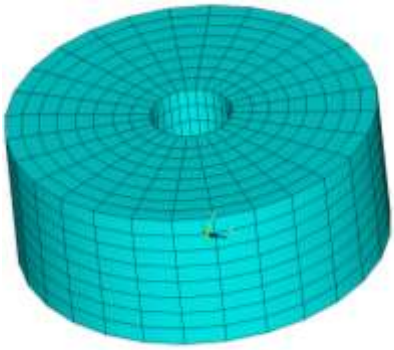

Fig. 4: Flange model type FEM-L for $h = 20$ mm

4 Elasticity of Bolted Joint Components

Bearing in mind that stiffness is the inverse of elasticity, the stiffness of the bolt c_s can be determined, based on the guidelines in VDI 2230 standard [55], as the sum of the inverse of the stiffnesses of the individual parts of the bolt c_{si}:

$$\frac{1}{c_s} = \sum_i \frac{1}{c_{si}} \tag{4}$$

The bolt stiffness values obtained for the different flange thicknesses h are summarised in Table 1. The bolt stiffness calculated in this way was adopted for all bolt joint models.

Table 1. Value of bolt stiffness as a function of flange thickness h

h [mm]	20	40	80
c_s [MN/mm]	0.434	0.284	0.168

The values of the flange stiffness c_p determined for the adopted bolted joint models and the individual flange thicknesses h are collected in Table 2. In the case of the VDI and FEM-L models, the linear stiffness values are given as calculation results, while in the case of the FEM-NL model, the stiffness values determined from the non-linear stiffness characteristics for $F_m = 20$ kN.

Based on the obtained bolt and flange stiffness values, elasticity diagrams were plotted. As the diagrams obtained are qualitatively similar, only an example of them is included in the paper, for a flange thickness of $h = 20$ mm (Figure 5).

Table 2. Value of flange stiffness as a function of its thickness h

h [mm]	$c_{p,VDI}$	$c_{p,FEM\text{-}L}$	$c_{p,FEM\text{-}NL}$
	[MN/mm]		
20	6.796	5.520	3.456
40	4.989	4.040	3.090
80	3.711	2.841	2.487

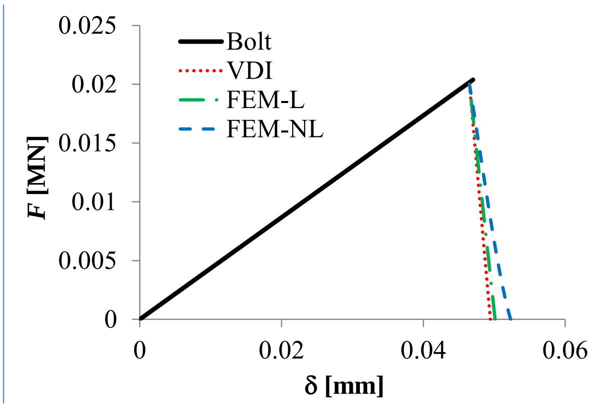

Fig. 5: Elasticity diagram for $h = 20$ mm

A quantitative evaluation of the resulting elasticity diagrams was made on the basis of the W_1 index given by the formula:

$$W_1 = \frac{c_{p,x} - c_{p,FEM-NL}}{c_{p,FEM-NL}} \cdot 100 \tag{5}$$

where: $c_{p,x}$ – flange stiffness value for linear models (x = VDI or FEM-L), $c_{p,FEM\text{-}NL}$ – linearised value of the flange stiffness for the FEM-NL model.

The W_1 index values determined for all cases of flange thickness are summarised in Table 3.

Table 3. Value of W_1 index as a function of flange thickness h

$h = 20$ mm		$h = 40$ mm	
$W_{1,\mathrm{VDI}}$ [%]	$W_{1,\mathrm{FEM\text{-}L}}$ [%]	$W_{1,\mathrm{VDI}}$ [%]	$W_{1,\mathrm{FEM\text{-}L}}$ [%]
96.6	59.7	61.5	30.7
$h = 80$ mm			
$W_{1,\mathrm{VDI}}$ [%]	$W_{1,\mathrm{FEM\text{-}L}}$ [%]		
49.2	14.2		

Disregarding the non-linearity of the contact layer can result in an overestimation of stiffness values of 49.2% to 96.6% for the VDI model and 14.2% to 59.7% for the FEM-L model. With increasing flange thickness, an increasingly better approximation of the stiffness determined for the linear FEM model to the stiffness determined for the non-linear FEM model is obtained.

Based on Eqs. (1) and (2), and for an assumed value of α = 0.1, the values of the working load in the bolt F_s were determined for the different flange models and thicknesses. The values of F_s are collected in Table 4.

Table 4. Value of working load as a function of its thickness *h*

h [mm]	$F_{s,VDI}$	$F_{s,FEM\text{-}L}$	$F_{s,FEM\text{-}NL}$
	[N]		
20	20120	20146	20223
40	20108	20131	20168
80	20087	20112	20127

A quantitative evaluation of the resulting working load values in the bolt was made on the basis of the W_2 index given by the formula:

$$W_2 = \frac{F_{s,x} - F_{s,FEM-NL}}{F_{s,FEM-NL}} \cdot 100 \quad (6)$$

where: $F_{s,x}$ – value of the working load in the bolt for linear models (x = VDI or FEM-L), $F_{s,FEM\text{-}NL}$ – value of the working load in the bolt for the FEM-NL model.

The W_2 index values determined for all cases of flange thickness are summarised in Table 5.

Table 5. Value of W_2 index as a function of flange thickness *h*

h = 20 mm		*h* = 40 mm	
$W_{2,\mathrm{VDI}}$ [%]	$W_{2,\mathrm{FEM\text{-}L}}$ [%]	$W_{2,\mathrm{VDI}}$ [%]	$W_{2,\mathrm{FEM\text{-}L}}$ [%]
-0.51	-0.38	-0.30	-0.18
h = 80 mm			
$W_{2,\mathrm{VDI}}$ [%]	$W_{2,\mathrm{FEM\text{-}L}}$ [%]		
-0.20	-0.07		

Neglecting the non-linearity of the contact layer can result in a slight underestimation of the working load in the bolt of 0.20% to 0.51% for the VDI model and 0.07% to 0.38% for the FEM-L model.

5 Conclusions

The analysis of bolted joint stiffness shows that neglecting the non-linearity of the contact layer has little effect on the variation of working loads in the bolt in a preloaded bolted joint. Since bolted joints are in practice usually calculated with significant safety factor values, it can be considered that the stress values induced in the joint by the working loads obtained according to linear models will not exceed the allowable stress values. The use of linear models for bolted joints is therefore justified, especially for engineering calculations, but also in scientific calculations where the aim is to achieve fast calculation results. In the future, the validity of the above conclusions can be tested for multi-bolted connections.

References:

[1] K. Miatliuk, A. Lukaszewicz, F. Siemieniako, Coordination method in design of forming operations of hierarchical solid objects, *Proceedings of the International Conference on Control, Automation and Systems*, Seoul, Korea, 14-17 October 2008, pp. 2724-2727, https://doi.org/10.1109/ICCAS.2008.4694220.

[2] A. Łukaszewicz, K. Miatliuk, Reverse engineering approach for object with free-form surfaces using standard surface-solid parametric CAD system, *Solid State Phenomena*, Vols. 147-149, 2009, pp. 706-711, https://doi.org/10.4028/www.scientific.net/SSP.147-149.706.

[3] J. Diakun, Recycling Product Model and Its Application for Quantitative Assessment of Product Recycling Properties, *Sustainability*, Vol. 16, No. 7, 2024, Paper No. 2880, https://doi.org/10.3390/su16072880.

[4] R. Grzejda, Modelling nonlinear multi-bolted connections: A case of operational condition, *Proceedings of the 15th International Scientific Conference 'Engineering for Rural Development 2016'*, Jelgava, Latvia, 25-27 May 2016, pp. 336-341, [Online]. https://www.iitf.lbtu.lv/conference/proceedings2016/Papers/N061.pdf (Accessed Date: October 1, 2024).

[5] P. Palenica, B. Powałka, R. Grzejda, Assessment of modal parameters of a building structure model, *Springer Proceedings in Mathematics & Statistics*, Vol. 181, 2016, pp. 319-325, https://doi.org/10.1007/978-3-319-42402-6_25.

[6] R. Grzejda, Impact of nonlinearity of the contact layer between elements joined in a multi-bolted system on its preload, *International Journal of Applied Mechanics and Engineering*, Vol. 22, No. 4, 2017, pp. 921-930, https://doi.org/10.1515/ijame-2017-0059.

[7] J. Kim, J.-C. Yoon, B.-S. Kang, Finite element analysis and modeling of structure

with bolted joints, *Applied Mathematical Modelling*, Vol. 31, No. 5, 2007, pp. 895-911, https://doi.org/10.1016/j.apm.2006.03.020.

[8] Z. Wang, C.-W. Fei, J.-J. Wang, Equivalent simulation of mechanical characteristics or parametric modeling of bolted joint structures, *Advances in Mechanical Engineering*, Vol. 9, No. 6, 2017, pp. 1-12, https://doi.org/10.1177/1687814017704360.

[9] R. Kumpati, W. Skarka, M. Skarka, Design optimization and failure analysis of natural composite sandwich T-joints under pulling load conditions, *Engineering Failure Analysis*, Vol. 164, 2024, Paper No. 108672, https://doi.org/10.1016/j.engfailanal.2024.108672.

[10] R. Verwaerde, P.-A. Guidault, P.-A. Boucard, A nonlinear finite element connector for the simulation of bolted assemblies, *Computational Mechanics*, Vol. 65, No. 6, 2020, pp. 1531-1548, https://doi.org/10.1007/s00466-020-01833-1.

[11] N. Tanlak, F. O. Sonmez, E. Talay, Detailed and simplified models of bolted joints under impact loading, *Journal of Strain Analysis for Engineering Design*, Vol. 46, No. 3, 2011, pp. 213-225, https://doi.org/10.1177/0309324710396997.

[12] M. R. Choudhury, S. Quayyum, K. M. Amanat, Modeling and analysis of a bolted flanged pipe joint subjected to bending, *Proceedings of the WSEAS International Conference on Engineering Mechanics, Structures, Engineering Geology*, Heraklion, Crete Island, Greece, 22-24 July 2008, pp. 1-9.

[13] K. Szopa, M. Iwaniec, J. Iwaniec, Modelling and identification of bolted truss structure with the use of design of experiment approach, *Structures*, Vol. 27, 2020, pp. 462-473, https://doi.org/10.1016/j.istruc.2020.05.047.

[14] S. Dominikowski, P. Bogacz, Determination of internal forces in end plates of simple end plate joints, *Technical Sciences*, Vol. 12, 2009, pp. 83-94, [Online]. https://uwm.edu.pl/wnt/technicalsc/tech_12/B08.pdf (Accessed Date: October 1, 2024).

[15] D. Mahaarachchi, M. Mahendran, Finite element analysis and design of crest-fixed trapezoidal steel claddings with wide pans subject to pull-through failures, *Engineering Structures*, Vol. 26, No. 11, 2004, pp. 1547-1559, https://doi.org/10.1016/j.engstruct.2004.05.007.

[16] L. Gödrich, F. Wald, Z. Sokol, To advanced modelling of end plate joints, *Journal of Civil Engineering, Environment and Architecture*, Vol. 30, No. 60, 2013, pp. 77-86, https://doi.org/10.7862/rb.2013.18.

[17] B. Blachowski, W. Gutkowski, Effect of damaged circular flange-bolted connections on behaviour of tall towers, modelled by multilevel substructuring, *Engineering Structures*, Vol. 111, 2016, pp. 93-103, https://doi.org/10.1016/j.engstruct.2015.12.018.

[18] R. Grzejda, Numerical investigation of the variability of bolt forces in a preloaded asymmetric multi-bolted connection under cyclical loading, *WSEAS Transactions on Applied and Theoretical Mechanics*, Vol. 18, 2023, pp. 68-74, https://doi.org/10.37394/232011.2023.18.7.

[19] R. Grzejda, Modeling the normal contact characteristics between components joined in multi-bolted systems, *WSEAS Transactions on Applied and Theoretical Mechanics*, Vol. 19, 2024, pp. 73-81, https://doi.org/10.37394/232011.2024.19.8.

[20] P. Dunaj, A. Archenti, Modeling the dynamic interaction between machine tools and their foundations, *Precision Engineering*, Vol. 89, 2024, pp. 451-472, https://doi.org/10.1016/j.precisioneng.2024.07.009.

[21] J. Aguirrebeitia, M. Abasolo, R. Avilés, I. F. de Bustos, General static load-carrying capacity for the design and selection of four contact point slewing bearings: Finite element calculations and theoretical model validation, *Finite Elements in Analysis and Design*, Vol. 55, 2012, pp. 23-30, https://doi.org/10.1016/j.finel.2012.02.002.

[22] G. S. Prinz, A. Nussbaumer, L. Borges, S. Khadka, Experimental testing and simulation of bolted beam-column connections having thick extended endplates and multiple bolts per row, *Engineering Structures*, Vol. 59, 2014, pp. 434-447, https://doi.org/10.1016/j.engstruct.2013.10.042.

[23] H.-Y. Hwang, Bolted joint torque setting using numerical simulation and experiments, *Journal of Mechanical Science and Technology*, Vol. 27, No. 5, 2013, pp. 1361-

1371, https://doi.org/10.1007/s12206-013-0317-2.

[24] B. Stankiewicz, Parametric analysis of stiffness of bolted end-plate connections of I beams using finite element method, *Journal of Civil Engineering, Environment and Architecture*, Vol. 30, No. 60, 2013, pp. 231-242, https://doi.org/10.7862/rb.2013.28.

[25] K. P. Raju, K. Bodjona, G.-H. Lim, L. Lessard, Improving load sharing in hybrid bonded/bolted composite joints using an interference-fit bolt, *Composite Structures*, Vol 149, 2016, pp. 329-338, https://doi.org/10.1016/j.compstruct.2016.04.025.

[26] S. Palit, S. K. Bhattacharyya, D. Maity, Behaviour of bolted rigid joint with endplate under localised fire scenario, *Journal of Constructional Steel Research*, Vol. 214, 2024, Paper No. 108484, https://doi.org/10.1016/j.jcsr.2024.108484.

[27] P. Pieczka, P. Iwicki, Rotational stiffness of a connection made using a single prestressed bolt, *Engineering Structures*, Vol. 321, 2024, Paper No. 118935, https://doi.org/10.1016/j.engstruct.2024.118935.

[28] Z. Wu, S. Zhang, S.-F. Jiang, Simulation of tensile bolts in finite element modeling of semi-rigid beam-to-column connections, *International Journal of Steel Structures*, Vol. 12, No. 3, 2012, pp. 339-350, https://doi.org/10.1007/s13296-012-3004-8.

[29] G. Yang, J. Hong, L. Zhu, B. Li, M. Xiong, F. Wang, Three-dimensional finite element analysis of the mechanical properties of helical thread connection, *Chinese Journal of Mechanical Engineering*, Vol. 26, No. 3, 2013, pp. 564-572, https://doi.org/10.3901/CJME.2013.03.564.

[30] H. Gong, J. Liu, X. Ding, Calculation of the effective bearing contact radius for precision tightening of bolted joints, *Advances in Mechanical Engineering*, Vol. 8, No. 9, 2016, pp. 1-8, https://doi.org/10.1177/1687814016668445.

[31] M. Gryniewicz, M. J. Roberts, J. M. Davies, Testing and analysis of a full-scale steel-framed building including the consideration of structure-cladding interaction, *Journal of Constructional Steel Research*, Vol. 181, 2021, Paper No. 106611, https://doi.org/10.1016/j.jcsr.2021.106611.

[32] X. Liu, S. Jin, M. Ming, C. Fan, H. Liu, D. J. Politis, M. Kopec, A high throughput in-situ measurement of heat transfer in successive non-isothermal forming of sheet alloys, *Journal of Manufacturing Processes*, Vol. 129, 2024, pp. 77-91, https://doi.org/10.1016/j.jmapro.2024.08.048.

[33] M. Abid, D. H. Nash, Relaxation behaviour of a gasketed and non-gasketed bolted flanged pipe joint – A comparative study, *WSEAS Transactions on Applied and Theoretical Mechanics*, Vol. 1, No. 2, 2006, pp. 239-246.

[34] A. Witek, Load analysis of multibolt joints concerning nonlinearity and friction, *Archives of Mechanical Technology and Automation*, Vol. 20, No. 2, 2000, pp. 131-144.

[35] Y. Chang, J. Ding, H. Fan, Interfacial micromechanics study on contact modeling for bolted joints, *Acta Mechanica*, Vol. 234, No. 8, 2023, pp. 3377-3396, https://doi.org/10.1007/s00707-023-03562-x.

[36] M. E. Abo-Elnor, Design and analysis of watertight bolted pressure chamber, *WSEAS Transactions on Applied and Theoretical Mechanics*, Vol. 11, 2016, pp. 129-135, [Online]. https://wseas.com/journals/articles.php?id=3700 (Accessed Date: October 1, 2024).

[37] E. Bernatowska, L. Ślęczka, Experimental and numerical investigation into failure modes of tension angle members connected by one leg, *Materials*, Vol. 14, No. 18, 2021, Paper No. 5141, https://doi.org/10.3390/ma14185141.

[38] P. Marek, J. Pawlicki, A. Mościcki, Tightness problems at the flange connection in transient temperature and high pressure condition, *Engineering Failure Analysis*, Vol. 133, 2022, Paper No. 105986, https://doi.org/10.1016/j.engfailanal.2021.105986.

[39] M. Ge, X. Cheng, W. Huang, R. Hu, Y. Cheng, Damage mode and load distribution of countersunk bolted composite joints, *Journal of Composite Materials*, Vol. 55, No. 13, 2021, pp. 1717-1732, https://doi.org/10.1177/0021998320976782.

[40] G. Xu, Y. Wang, Y. Du, W. Zhao, L. Wang, Static strength of friction-type high-strength bolted T-stub connections under shear and compression, *Applied Sciences*, Vol. 10, No. 10, 2020, Paper No. 3600, https://doi.org/10.3390/app10103600.

[41] O. Khandel, M. F. Tamimi, M. Soliman, B. W. Russell, C. D. Waite, Reliability

assessment of connections with slip-critical bolts and fillet welds in combination, *Journal of Constructional Steel Research*, Vol. 188, 2022 Paper No. 107036, https://doi.org/10.1016/j.jcsr.2021.107036.

[42] P. Jaszak, Prediction of the durability of a gasket operating in a bolted-flange-joint subjected to cyclic bending, *Engineering Failure Analysis*, Vol. 120, 2021, Paper No. 105027, https://doi.org/10.1016/j.engfailanal.2020.105027.

[43] Y. Yang, W. Liu, M. Gong, G. Zhang, Analysis of load and stress distribution of a bolted joint composite plate, *Proceedings of the Institution of Mechanical Engineers, Part C: Journal of Mechanical Engineering Science*, Vol. 237, No. 17, 2023, pp. 3968-3976, https://doi.org/10.1177/09544062221149322.

[44] M. Klasztorny, K. P. Zajac, D. B. Nycz, GFRP composite footbridge series with multi-box cross section – Part 2: Local detailed design, *Composite Structures*, Vol. 253, 2020, Paper No. 112799, https://doi.org/10.1016/j.compstruct.2020.112799.

[45] D. Kukla, A. Kozlowski, Parametric study of steel flush and extended end-plate joints under column loss scenario, *Engineering Structures*, Vol. 237, 2021, Paper No. 112204, https://doi.org/10.1016/j.engstruct.2021.112204.

[46] O. M. U. Eraliev, Y.-H. Zhang, K.-H. Lee, C.-H. Lee, Experimental investigation on self-loosening of a bolted joint under cyclical temperature changes, *Advances in Mechanical Engineering*, Vol. 13, No. 8, 2021, pp. 1-8, https://doi.org/10.1177/16878140211039428.

[47] P. Wang, J. Pan, Z. Wang, B. Li, J. Qin, Experimental and numerical investigation of stiffened angle connection in a minor axis, *Science Progress*, Vol. 103, No. 4, 2020, pp. 1-27, https://doi.org/10.1177/0036850420973521.

[48] Y. Rongqian, Z. Xuejun, Experimental study on the seismic behavior of concentrically braced steel frames with extended end-plate bolted connections, *Science Progress*, Vol. 103, No. 3, 2020, pp. 1-21, https://doi.org/10.1177/0036850420952289.

[49] M. Feldmann, J. Naumes, D. Pak, Load-deformation behaviour of preloaded bolts in ring flange connections with bridged gaps with regard to a fatigue behaviour prediction (in German), *Stahlbau*, Vol. 80, No. 1, 2011, pp. 21-29, https://doi.org/10.1002/stab.201001386.

[50] N. Stranghöner, D. Jungbluth, V. Hüller, G. Machura, Tightening of bolted connections according to Eurocode 3 and DIN EN 1090-2 (in German), *Stahlbau*, Vol. 85, No. 5, 2016, pp. 327-335, https://doi.org/10.1002/stab.201610377.

[51] P. Jaszak, Optimized design of a semimetal gasket operating in flange-bolted joints, *Open Engineering*, Vol. 11, No. 1, 2021, pp. 56-66, https://doi.org/10.1515/eng-2021-0004.

[52] F. Wald, M. Vild, M. Kuříková, J. Kabeláč, D. Sekal, N. Maier, L. Da Silva Seco, M. Couchaux, Component based finite element design of steel joints, *Civil Engineering Design*, Vol. 2, No. 3, pp. 78-89, https://doi.org/10.1002/cend.202000015.

[53] S.-A. Wang, M. Zhu, F. Wu, T.-X. Liang, Z.-Q. Shao, Y.-L. Liu, Analysis of pressure distribution of the bolted joints based on the finite element method, *International Journal of Steel Structures*, Vol 23, No. 2, 2023, pp. 586-598, https://doi.org/10.1007/s13296-023-00714-6.

[54] K. Grudziński, R. Kawiak, Determination of elastic compliance of joined elements in an axisymmetric bolted joint (in Polish), *Przegląd Mechaniczny*, Vol. 49, No. 17, 1990, pp. 10-14.

[55] VDI 2230, Systematic calculation of highly stressed bolted joints, Joints with one cylindrical bolt (in German), 2015, [Online]. https://www.vdi.de/en/home/vdi-standards/details/vdi-2230-blatt-1-systematic-calculation-of-highly-stressed-bolted-joints-joints-with-one-cylindrical-bolt (Accessed Date: October 1, 2024).

[56] W. Lori, H. Gläser, Calculation of plate flexibility for bolted connections (in German), *Konstruktion*, Vol. 42, No. 9, 1990, pp. 271-277.

[57] PN-EN 1591-1: 2014-04, Flanges and their joints, Design rules for gasketed circular flange connections, Part 1: Calculation, [Online]. https://sklep.pkn.pl/pn-en-1591-1-2014-04e.html (Accessed Date: October 1, 2024).

[58] PN-EN ISO 7091: 2003, Plain washers, Normal series, Product grade C, [Online]. https://sklep.pkn.pl/normy/pn-en-iso-7091-2003p.html (Accessed Date: October 1, 2024).

[59] Y. Fu, Y.-S. Wang, Y. Fu, Wrinkling of a film/substrate bilayer with periodic material properties: An assessment of the Winkler foundation model, *International Journal of Non-Linear Mechanics*, Vol. 166, 2024, Paper No. 104815, https://doi.org/10.1016/j.ijnonlinmec.2024.104815.

[60] O. Soukaina, M. Hamid, H. Bachir, Numerical investigation of member stiffness in composite sandwich bolted connections, *Strength of Materials*, Vol. 55, No. 5, 2023, pp. 986-1005, https://doi.org/10.1007/s11223-023-00590-9.

Contribution of Individual Authors to the Creation of a Scientific Article (Ghostwriting Policy)

The author contributed in the present research, at all stages from the formulation of the problem to the final findings and solution.

Sources of Funding for Research Presented in a Scientific Article or Scientific Article Itself

No funding was received for conducting this study.

Conflict of Interest

The author has no conflicts of interest to declare.